

Electronic structure and transport in liquid Te[†]

Morrel H. Cohen

The James Franck Institute and Department of Physics, The University of Chicago, Chicago, Illinois 60637

Joshua Jortner

Department of Chemistry, Tel-Aviv University, Tel-Aviv, Israel

(Received 6 August 1975)

In this paper we explore the consequence of bonding inhomogeneities on the structural, magnetic, and electrical transport properties of liquid Te in the temperature range 675–1250 K. Assuming that the short correlation length b is of the order of several interatomic separations, local electronic structure and local response functions are defined. The volume fraction C of the metallic regions was determined from Knight-shift data. The enhancement factor for the spin-lattice relaxation rate is proportional to C^{-1} , in good agreement with the experimental data. The electrical conductivity and the Hall coefficient were analyzed in terms of an effective-medium theory.

We have recently advanced a physical picture for a continuous metal-nonmetal transition in some disordered materials.^{1–5} It was pointed out that local electronic structure and transport properties can be defined provided that the short correlation length^{5,6} b for fluctuation is long compared to the phase coherence length l of the conduction electrons. In the vicinity of a metal-nonmetal transition, the local electronic structure depends sensitively on the local electronic configuration.^{5–7} As a consequence of the fluctuations, the material becomes microscopically inhomogeneous as regards transport. For sufficiently large values of b , tunneling corrections⁸ can be disregarded,^{2,4,5} and local transport theory⁶ is applicable.

We have examined two materials in some detail with the aid of this picture, expanded liquid mercury² and metal-ammonia solutions.⁴ In the former case we deal with a unimodal distribution of density fluctuations, in the latter case with a bimodal distribution of concentration fluctuations. In both cases we were able to advance strong arguments for the existence of microscopic inhomogeneities to fit the transport data accurately to the theory of inhomogeneous transport.^{9–13} We have developed this theory,^{4,12,13} to extract the volume fraction of metallic regions within the inhomogeneous material and to estimate b . In the present paper we continue this program and report a parallel investigation of liquid Te, of which a preliminary account has appeared.¹

Liquid Te provides an example of inhomogeneities originating from bonding modifications in a one-component system. In liquid Te, Cabane and Friedel¹⁴ have already proposed a state of mixed coordination in order to explain structural¹⁵ and magnetic resonance data.^{16,17} They suggest the existence of regions of threefold coordination which are metallic mixed with regions of twofold coordination which are semiconducting. Using

crude chemical terms, in the twofold coordinated state a lone pair does not participate in bonding. In the threefold coordinated state, the lone pair electrons become bonding electrons, one being tied up in the additional bond, leaving one free. A more sophisticated analysis would yield more than one electron free to conduct.

As is evident from Fig. 1, a metallic regime characterized by a conductivity^{18–20} $\sigma \approx 2700 (\Omega \text{ cm})^{-1}$, which is on the borderline between propagation^{21–23} and diffusion,^{24–27} fits the transport data above about 1100 K; this limit will be discussed below. In the temperature range $650 < T < 1250$ K, in which the liquid has been studied, the conductivity varies in the range^{18–20} 2700 to 860 $(\Omega \text{ cm})^{-1}$ while the Hall mobility^{28–31} remains constant within 5%. Mott^{32–36} and Warren¹⁷ have utilized the Knight-shift data K , Fig. 1, to derive the g parameter^{26,32–36} and conclude that the Mott-Friedman relation $\sigma \propto \mu g^2$ in the form $\sigma = A' K^2$ is obeyed, providing evidence for the applicability of the diffusion regime. We note empirically, however, that an alternative, linear relation $\sigma = A'' K - B''$ also holds over the temperature range $675 < T < 950$ K, Fig. 2. More important, the applicability of the diffusion regime would require μ to vary by about 60%, according to Friedman's theory,²⁷ in the form utilized by Even and Jortner³⁷ and by us,² while the propagation regime would require μ to vary by about a factor of ~ 3.1 . Both predicted variations are at least an order of magnitude larger than what is observed. We conclude again that neither of the conventional metallic transport regimes is consistent with the transport data. Accordingly, we apply our picture of transport in microscopically inhomogeneous material to liquid Te.

Because the configuration parameter is the coordination number for each atom, the correlation length b must be at least one interatomic separation, 2.8 Å, in the threefold coordinated configur-

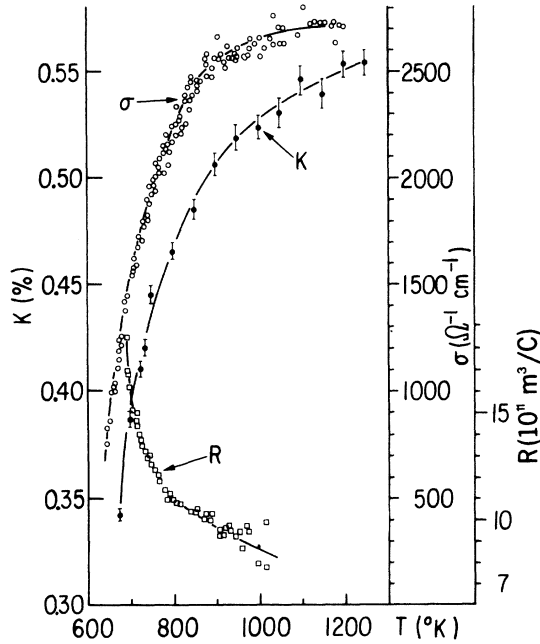


FIG. 1. Temperature dependence of the electrical conductivity σ (Ref. 20), the Hall coefficient R (Ref. 31), and the Knight shift K (Ref. 17) for liquid Te. Error bars on K data (Ref. 17) indicate experimental uncertainty. Accuracy of σ data (Ref. 20) is 5% and of R data (Ref. 31) is 7%.

ation. The formula for σ for an isotropic metal in the propagation regime is Ne^2l/p_F , where N is the electron density, p_F is the Fermi momentum, and l is the mean free path. Assuming three conduction electrons per atom and a conductivity of $2700 (\Omega \text{ cm})^{-1}$ in the metallic regions leads to a value of 1.2 for $k_F l$. In expanded liquid Hg the transition from the propagation to the diffusion regime occurs when $k_F l$ is 2.3. Thus the conductivity is inconsistent with the propagation regime. The Hall constant¹⁴ R is such that $R/R_{FE} = 1.2$ where R_{FE} is the free-electron value. This plus the conductivity implies that electrons in metallic liquid Te are in the diffusion regime. l can therefore not be regarded simply as a mean free path but must be considered a phase coherence length. From our experience²⁷ with Hg we expect that $l \leq (2.3k_F)^{-1} = 0.8 \text{ \AA}$, and the condition $b > l$ is well met, as $b/l > 3.5$. We can then consider the medium as a submacroscopically inhomogeneous random mixture of regions of radius b which can be treated semiclassically as locally uniform. The electron wave function does not actually go to zero within the excluded region. Nevertheless, it can become small enough there to be unimportant in a variety of contexts.

Accordingly, we define an allowed volume fraction $C(E)$ as being that fraction of the total volume

of the material actually allowed to electrons of energy E . Now, the Weyl theorem³⁸ tells us that as long as the shorter of the de Broglie wavelengths (or the phase coherence length) is sufficiently small compared to the dimensions of the allowed regions, the density of states will be independent of the geometry of the allowed regions and of the boundary conditions presented by the forbidden regions and proportional to the allowed volume. Thus we may take^{1-5,8} as an approximate definition of $C(E)$,

$$n(E) = n_0(E)C(E), \quad (1)$$

where $n_0(E)$ is the density of states per unit volume of a metallic region of macroscopic extent, and $n(E)$ is the actual density of states of the microscopically inhomogeneous material. Defined in this way, $C(E)$ allows properly for penetration into the excluded regions.

The quantity $C(E_F) \equiv C$ is the volume fraction of the material from which contributions of the electrons at the Fermi energy of the metallic regions to the physical properties arise. Similarly, $1 - C(E_F) \equiv 1 - C$ is the volume fraction from which nonmetallic contributions originate.

Experimental paramagnetic volume susceptibility χ_p or Knight-shift K data can be utilized to obtain C . Because local-field corrections are negligible in χ_p , effective-medium theory for this response function is unnecessary, and we can write

$$\chi_p = C\chi_0 + (1 - C)\chi_1, \quad (2)$$

where χ_0 and χ_1 are the metallic and the semicon-

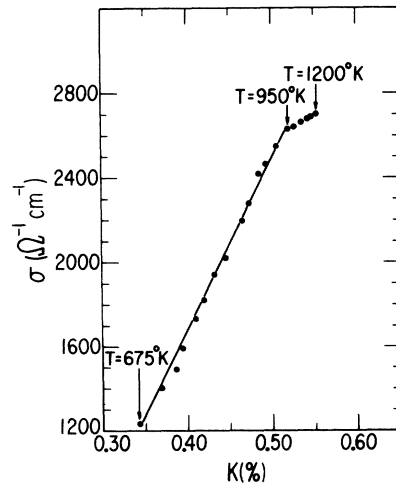


FIG. 2. Plot of σ vs K for liquid Te with the temperature an implicit variable. Note that in the temperature range $675 < T < 950 \text{ K}$ a linear σ vs K relation holds.

ducting paramagnetic susceptibility, respectively. We now turn to the relation between the Knight shift and the volume susceptibility. The configuration relaxation time is much shorter than the uncertainty time for the Knight shift, so we are dealing with the limit of extreme motional narrowing for the nuclear resonance. Consequently, the experimental Knight shift is the mean of the shifts K_0 in the metallic regions, and K_1 in the semiconducting regions, weighted by the proportion each region contributes to the nuclear volume susceptibility χ_T^n :

$$K = K_0 \frac{\chi_0^n}{\chi_T^n} C + K_1 \frac{\chi_1^n}{\chi_T^n} (1 - C), \quad (3)$$

where χ_0^n and χ_1^n are the nuclear volume susceptibility in the metallic and nonmetallic regions, respectively. As each nuclear susceptibility is proportional to the corresponding nuclear number density, Eq. (3) can be rewritten as

$$\bar{N}K = K_0 N_0 C + K_1 N_1 (1 - C), \quad (4)$$

where \bar{N} is the mean number density, and N_0 and N_1 are that quantity in the metallic and in the semiconducting regions, respectively. Comparing (2) and (4) we see that $\bar{N}K$ and χ are linearly related. Because thermal-expansion effects are relatively small,³⁹ ($\sim 7\%$) in the temperature range 492–1000°C, the number densities \bar{N} , N_0 , and N_1 in Eq. (4) can be treated as constants. There results the linear K vs χ relation reported by Warren.¹⁷ Further, ignoring small differences among N_0 , N_1 , and \bar{N} , and neglecting K_1 , we obtain

$$K = K_0 C. \quad (5)$$

Equation (5) permits us to determine the C scale from the Knight-shift data in the temperature range 675–1250 K, Fig. 1. In our previous work¹ we have extrapolated Warren's data¹⁷ to a saturation value of 0.560% at 1350 K and used that as K_0 . A more careful examination of the available conductivity and magnetic data, Figs. 1 and 2, reveals that σ and K exhibit weak temperature dependence above ~ 1000 K. As in our previous work¹ we first neglect the temperature dependence of K_0 , setting $C = 1$ at 950 K. We then apply Eq. (5) together with the experimental value of 0.517% for K at 950 K and use that as K_0 . The resulting values of C vs T are shown in Fig. 3. Next, we account for the temperature dependence of the Knight shift in the metallic regions. We can safely assume that above 1100 K the metallic diffusion regime applies and $C = 1$. The temperature dependence of the Knight shift $K \equiv K_0$ in the range $1100 \leq T \leq 1250$ K, which from the best fit of Warren's data is

$$K_0(T) = 0.557[1 + \gamma(T - 1250)]\%, \quad (6)$$

$$\gamma = 1.6 \times 10^{-4} \text{ K}^{-1},$$

originates from volume-expansion effects in the homogeneous metallic material. The metallic Knight shift is

$$K_0(T) = (\chi_0/N_0)^{\frac{2}{3}} \pi \langle \psi(0)_F^2 \rangle_{av}, \quad (7)$$

where $\langle \psi(0)_F^2 \rangle_{av}$ is the probability for the conduction electrons at the nucleus averaged over the Fermi surface. The volume susceptibility has the Pauli form $\chi_0 = \mu_B^2 n_0(E_F)$, where μ_B is the Bohr magneton. The temperature dependence of K_0 is

$$\gamma = \frac{d \ln K_0}{dT} = -\frac{d \ln N_0}{dT} + \frac{d}{dT} \{ \ln [n_0(E_F) \langle \psi(0)_F^2 \rangle_{av}] \}. \quad (8)$$

Density data are available³³ in the temperature range 668–1273 K. From the density data³⁹ for $1100 < T < 1273$ K corresponding to the metallic regime, we estimate $-(d \ln N_0/dT) = 1.5 \times 10^{-4} \text{ K}^{-1}$, which is close to the value of γ , Eq. (6), obtained from the magnetic data. Both the magnetic and volume-expansion data are not sufficiently accurate to extract the contribution to γ originating from the second term on the right-hand side of Eq. (8). Equation (6) is now applicable for the evaluation of the local Knight shift $K_0(T)$ within the metallic regions in the microscopically inhomogeneous materials at $T < 1100$ K. The values of C resulting from use of Eqs. (5) and (6) are shown as a function of temperature in Fig. 3. The temperature dependence of K_0 has only a minor effect ($< 4\%$) on the C scale. We also note that C only changes from 1.00 to 0.98 between 1100 and 950 K, so that the boundary of the inhomogeneous regime is spread over 150 K, or so.

The C scale for Te permits us to clear up an

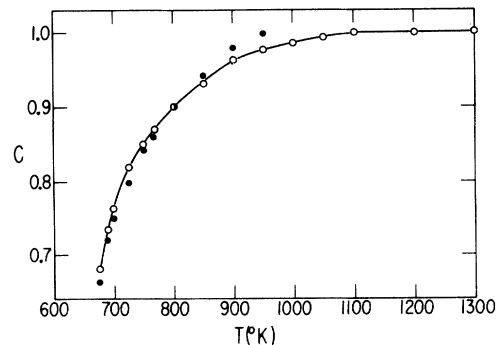


FIG. 3. C scale for liquid Te determined from Warren's Knight-shift data (Ref. 17): O: Eq. (5) with K_0 given by Eq. (6); ●: $C = 1$ at 950 K, utilizing Eq. (5) with $K_0 = 0.517$.

interesting puzzle concerning the origin of the relaxation-rate enhancement observed by Warren.¹⁷ In the case of extreme motional narrowing, the relaxation rate is given by an equation analogous to (3),

$$\frac{1}{T_1} = \left(\frac{1}{T_{1/0}}\right) \frac{\chi_0^n}{\chi_T^n} C + \left(\frac{1}{T_{1/1}}\right) \frac{\chi_1^n}{\chi_T^n} (1 - C). \quad (9)$$

The relaxation rate in the semiconducting regions can be safely neglected so that, ignoring the difference between N_0 and \bar{N} , Eq. (9) reduces to

$$1/T_1 = (1/T_{1/0})C. \quad (10)$$

Warren defines¹⁷ the relaxation-rate enhancement via the Korringa relation as

$$\eta = (1/T_1)/(1/T_1)_{\text{Korr}}, \quad (11)$$

$$(1/T_1)_{\text{Korr}} \propto K^2, \quad (12)$$

$$\eta \propto (1/T_1)K^{-2}. \quad (13)$$

Substituting (5), and (10) into (13) gives

$$\eta = \eta_0 C^{-1}, \quad (14)$$

where η_0 is the enhancement for the metallic regions. Equation (14) fits Warren's data for η to within experimental error, as shown in Fig. 4, yielding a value of 1.00 for η_0 . Mott⁴⁰ was the first to give Eq. (14) for η based on our picture of Te; however, his statement that Eq. (14) does not fit Warren's data is unjustified. In fact, the fit to Eq. (14) is superior to the fit obtained by using $\sigma \propto K^2$, $\eta \chi \bar{\sigma}^{-1}$ proposed by Warren.¹⁷ We conclude that the magnetic data are satisfactorily interpreted via our model.

We are now in a position to analyze the transport data.^{18-20,28-31} As the temperature range for which data are available spans the range $0.6 < C < 1$, there is no need to go beyond effective-medium theory (EMT). Moreover, as $2b/l \geq 7$, there is no need to introduce boundary scattering corrections.⁴¹ The EMT can be put into the form⁹⁻¹²

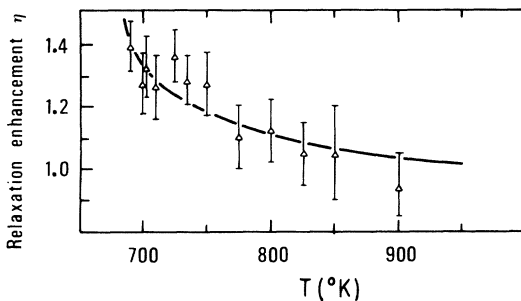


FIG. 4. Relaxation-rate enhancement η as a function of temperature. The solid line represents the prediction of Eq. (11) with $\eta_0 = 1.00$. The experimental points were obtained from Warren's work (Ref. 17).

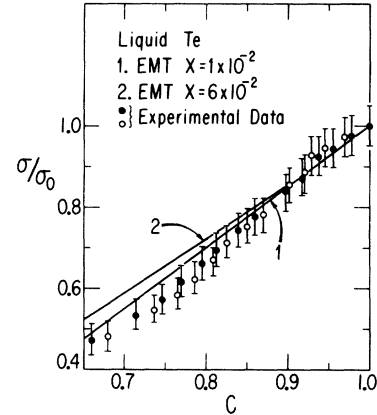


FIG. 5. Analysis of the experimental conductivity data for liquid Te (Ref. 20) in the inhomogeneous regime $T < 1100$ K in terms of the effective-medium theory (EMT). Analysis 1: C from Eqs. (5) and (6), σ_0 from Eq. (16) (\circ); analysis 2: $C = 1$ at 950 K, $\sigma_0 = 2620 \Omega \text{ cm}^{-1}$, $C = K/0.517$ (\bullet).

with σ_0 and σ_1 the local metallic and semiconducting conductivities, respectively. For a high-temperature material like liquid Te with a semiconducting gap of the order of 0.5 eV we expect a conductivity ratio of $10^{-2} < x < 10^{-1}$, which reinforces the validity of the EMT.¹¹

The conductivity data used derive from several sources.¹⁸⁻²⁰ The experimental data²⁰ were taken from the smoothed σ vs T curve of Fig. 1. In the

$$\begin{aligned} \sigma &= f\sigma_0, \\ f &= f(C, x) = a + (a^2 + \frac{1}{2}x)^{1/2}, \\ a &= \frac{1}{2}[(\frac{3}{2}C - \frac{1}{2})(1-x) + \frac{1}{2}x], \\ x &= \sigma_1/\sigma_0, \end{aligned} \quad (15)$$

analysis of these data we have first assumed that σ_0 and K_0 are independent of temperature. The experimental conductivity data were normalized to the value of σ at 950 K, $\sigma_0 = 2620 (\Omega \text{ cm})^{-1}$, and $C = K/0.517$. Next, we have accounted for the temperature dependence of σ_0 by utilizing a least-square fit of Perron's data²⁰ in the temperature range 1100–1200 K, where $C = 1$, which results in

$$\begin{aligned} \sigma_0(T) &= 2700[1 + \delta(T - 1200)] (\Omega \text{ cm})^{-1}, \\ \delta &= 9 \times 10^{-5} \text{ K}^{-1}. \end{aligned} \quad (16)$$

The C scale is now determined from Eqs. (5) and (6). The normalized conductivity data are plotted versus C in Fig. 5 with appropriate error bars.

The temperature effects on K_0 and σ_0 do not modify the relation of σ/σ_0 to C , within the accuracy of the experimental data. In Fig. 5 we show the fit of the experimental data to the EMT, Eq. (15), for x values in the range $10^{-2} \leq x \leq 10^{-2}$, as appropriate for a high-temperature material.

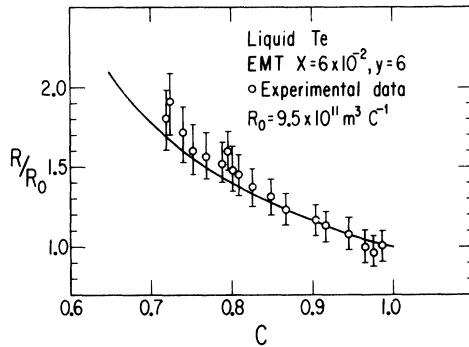


FIG. 6. Analysis of the Hall-effect data for liquid Te in terms of the effective-medium theory (EMT). Experimental Hall data from Ref. 31.

The fit to σ/σ_0 is within the uncertainty of the experimental data. We note that because σ_1 has the temperature dependence appropriate to a small-gap semiconductor, x decreases with temperature. Once x decreases below 10^{-2} , however, there is no further effect on σ/σ_0 for C in the present range.

EMT yields for the Hall coefficient R and for the Hall mobility μ ,

$$\begin{aligned} g &= g(x, y, f) = \mu/\mu_0 = [1 - B(1 - xy)]f^{-1}, \\ h &= h(x, y, f) = R/R_0 = [1 - B(1 - xy)]f^{-2}, \\ B &= \frac{(2f+1)^2(1-C)}{(2f+1)^2(1-C) + (2f+x)^2C}, \\ y &= \mu_1/\mu_0. \end{aligned} \quad (17)$$

The Hall-effect data used also derive from several sources.²⁸⁻³¹ They are shown in Fig. 6, together with a fit to EMT with the parameters $R_0 = 9.5 \times 10^{11} \text{ m}^3/\text{C}$, $x = 6 \times 10^{-2}$, and $y = 6$. The fit to the EMT is within the experimental error.

The fits to σ and R represent a vast improvement over the conventional homogeneous transport theories, metallic propagation or diffusion, which led to order of magnitude discrepancies.

Cabane and Friedel¹⁴ have estimated the fraction of threefold coordinated Te atoms from the ob-

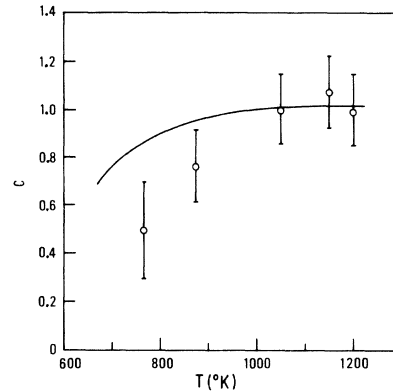


FIG. 7. Comparison between the fraction of threefold-coordinated Te atoms (circles with error bars) estimated (Ref. 14) from the radial distribution functions at different temperatures (Ref. 15) and the C scale (solid line) obtained from Knight-shift data.

served radial distribution functions.¹⁵ That number should be approximately equal to our estimate of C from the Knight shift. We plot both in Fig. 7 with error bars and note that there is adequate agreement considering the inaccuracy of the former quantity.

In sum, the structural, magnetic, and transport data are in accord with each other within the framework provided by the Cabane Friedel model¹⁴ of bonding inhomogeneities and our theories of the consequences of such inhomogeneities for the electronic properties.

It should be pointed out that Te is not the only material which shows such a continuous metal-nonmetal transition with temperature. Se, Se-Te alloys,²⁰ and some chalcogenide glasses all show similar characteristic temperature dependences of σ . Unfortunately, the data are as yet insufficient for a detailed quantitative analysis of the sort done here.

We are indebted to Dr. J. C. Perron, Dr. W. W. Warren, and Dr. J. E. Enderby for supplying us with their detailed experimental results.

¹Based on research supported in part by the ARO D, the Louis Block Fund and the Materials Research Laboratory of the National Science Foundation at the University of Chicago, and by the U.S.A.-Israel Binational Science Foundation at Tel-Aviv University.

¹Morrel H. Cohen and J. Jortner, *Phys. Rev. Lett.* **30**, 699 (1973).

²Morrel H. Cohen and J. Jortner, *Phys. Rev. A* **10**, 978 (1974).

³J. Jortner and Morrel H. Cohen, *J. Chem. Phys.* **58**, 5170 (1973).

⁴J. Jortner and Morrel H. Cohen, *Phys. Rev. B* (to be published).

⁵(a) Morrel H. Cohen and J. Jortner, in *Proceedings of*

the Fifth International Conference on Amorphous and Liquid Semiconductors (Taylor and Francis, London, 1974), p. 167; (b) *J. Phys.* **35**, C4-345 (1974).

⁶Morrel H. Cohen and J. Jortner, in *Proceedings of the International Conference on Amorphous and Liquid Metals*, edited by (Univ. of Mexico Press, Mexico City, to be published).

⁷Morrel H. Cohen and J. Sak, *J. Non-Cryst. Solids* **8-10**, 696 (1972).

⁸N. F. Mott, *Phys. Rev. Lett.* **31**, 466 (1973).

⁹D. A. G. Bruggeman, *Ann. Phys. (Leipz.)* **24**, 636 (1935).

¹⁰V. I. Odelevskii, *J. Tech. Phys. (USSR)* **21**, 678 (1951).

- ¹⁴S. Kirkpatrick, Phys. Rev. Lett. 27, 1722 (1971).
¹²Morrel H. Cohen and J. Jortner, Phys. Rev. Lett. 30, 696 (1973).
¹³Morrel H. Cohen and J. Jortner (unpublished).
¹⁴B. Cabane and J. Friedel, J. Phys. 32, 73 (1971).
¹⁵G. Tourand and M. Breuil, C. R. Acad. Sci. B 270, 109 (1970).
¹⁶B. Cabane and C. Froidevaux, Phys. Lett. A 29, 512 (1969).
¹⁷W. W. Warren, Phys. Rev. B 6, 2522 (1972).
¹⁸A. H. Epstein, H. Fritzsche, and K. L. Horovitz, Phys. Rev. 107, 412 (1957).
¹⁹M. Cutler and E. C. Mallon, J. Chem. Phys. 37, 2677 (1962).
²⁰J. C. Perron, in *Conduction in Low Mobility Materials*, edited by N. Klein, D. S. Tannhauser, and M. Pollak (Taylor and Francis, London, 1972), p. 243; and private communication.
²¹J. M. Ziman, Philos. Mag. 6, 1013 (1961).
²²T. E. Faber, Adv. Phys. 16, 578 (1967).
²³T. E. Faber, Adv. Phys. 15, 547 (1966).
²⁴A. F. Ioffe and A. R. Regel, Prog. Semicond. 4, 237 (1960).
²⁵Morrel H. Cohen, J. Non-Cryst. Solids 4, 391 (1970).
²⁶N. F. Mott, Adv. Phys. 16, 49 (1967).
²⁷L. Friedman, J. Non-Cryst. Solids 6, 329 (1971).
²⁸G. Busch and T. Tietche, Phys. Kondens. Mater. 1, 78 (1963).
²⁹J. C. Perron, Adv. Phys. 16, 657 (1967).
³⁰J. E. Enderby and L. Walsh, Philos. Mag. 14, 991 (1966).
³¹J. C. Perron, Rev. Phys. App. 5, 611 (1970), and (private communication).
³²N. F. Mott, Philos. Mag. 17, 1259 (1966).
³³N. F. Mott, Philos. Mag. 26, 1015 (1972).
³⁴Morrel H. Cohen, H. Fritzsche, and S. R. Ovshinsky, Phys. Rev. Lett. 22, 1065 (1969).
³⁵N. F. Mott, Philos. Mag. 24, 1 (1971).
³⁶N. F. Mott, Philos. Mag. 19, 835 (1969).
³⁷U. Even and J. Jortner, Phys. Rev. B 8, 2538 (1973).
³⁸H. Weyl, Math. Ann. 71, 441 (1912).
³⁹V. M. Glazov, S. N. Chizhevskaya, and N. N. Glagoleva, *Liquid Semiconductors* (Plenum, New York, 1969).
⁴⁰N. F. Mott, Philos. Mag. 29, 613 (1974).
⁴¹T. P. Eggarter, Phys. Rev. A 5, 2496 (1972).